Lasermethoden in der Strömungsmesstechnik
3. – 5. September 2013, München

Application of generalized rainbow patterns for the measurement of spheroidal droplets

Haitao Yu[1,*], Feng Xu[2], and Cameron Tropea[1,3]
[1] Institute of Fluid Mechanics and Aerodynamics, [3]Center of Smart Interfaces,
Technische Universität Darmstadt, Petersenstraße 17, 64287 Darmstadt, Germany
[2] Joint Institute for Regional Earth System Science and Engineering,
University of California, Los Angeles, CA 90095, USA
* Corresponding author: hyu@sla.tu-darmstadt.de

Keywords: Airy theory, Generalized rainbow pattern, Optical caustic, Vector ray tracing

Abstract

Generalized rainbow patterns from spheroidal water droplets are measured in experiment. Based on the generalized rainbow patterns and Airy theory, the refractive index and equatorial diameter of spheroidal water droplets can be determined. It is shown that absolute error of the refractive index is less than 0.5×10^{-4} and of the droplet diameter 5%. Furthermore, the relation between the curvature of the rainbow fringes and the aspect ratio of spheroidal water droplets is shown. Then the aspect ratio of spheroidal droplets is inferred from the corresponding generalized rainbow patterns with relative errors lying between -1% and 1%.

Introduction

Small particles play an important role in fields of science and engineering, e.g. in meteorology, environmental monitoring, spray, combustion research, chemical engineering. Liquid particles (droplets) exist in the atmosphere as cloud, fog and rain and in spray systems. Under aerodynamic or gravity forces, the droplets can be deformed from being spherical to being spheroidal. Understanding their light scattering properties is an important basis for developing optical diagnostic technique to characterize deformed droplets in terms of refractive index, size, shape and orientation, as well as evaluating errors arising from the spherical assumption made in many existing measurement techniques. According to a recent review in Ref. [1], optical particle characterization techniques are classified as direct imaging, intensity or intensity ratio, interferometry, time shift, pulse delay and Raman scattering, according to measurement principles. Interferometric techniques such as phase Doppler [2] and interferometric particle imaging [3] offer perhaps the most accurate determination of droplet size; however both techniques are sensitive to non-sphericity of the droplet. Although alternative optical techniques, such as the time shift technique [4], appear to be less sensitive to the droplet deformation in estimating droplet size [5], it is still necessary to have a quantitative access to the droplet deformation for exact size measurements. For characterizing spherical particle in terms of size and temperature, standard rainbow thermometry technique was developed [6]. This technique was generalized to global rainbow thermometry [7-9], yet still on the assumption that non-spherical droplets provide a uniform background; hence do not influence the interference pattern. On the basis of generalized rainbow patterns from spheroidal droplets, the refractive index and equatorial diameter of the spheroidal water droplet are

measured [10]. Nonetheless, none of the above methods are readily available for droplet non-sphericity measurements.

For further improvement and advancement of the optical techniques, the interpretation of light scattering from particles is a pre-requisite. For spherical and oblate spheroidal droplets, optical caustics were observed in far-field light scattering characterized by the generalized rainbow patterns around the first and higher-order rainbow angles. The generalized rainbow patterns include fold, cusp, swallowtail, butterfly, hyperbolic umbilic and symbolic umbilic diffraction catastrophes etc. in the language of catastrophe optics [11]. The hyperbolic umbilic diffraction catastrophe in the first rainbow region of spheroidal water droplet was first observed by Marston and Trinh [12]. The caustic structures were successfully described by some approximated theoretical models [13-20]. Most notably, Nye [20] studied the landmark features of the far-field caustics including hyperbolic umbilic foci, lip events and symbolic umbilic based on geometrical optics. The optical caustics were also observed in the scattering with white light illumination [21-22], in higher-order rainbow regions of scattering of light by oblate water droplet [23-25], and inside of liquid droplets [26]. Recently, Lock and Xu [27] developed Debye series to analyze the formation of rainbow caustic also called fold in catastrophe optics [11], transverse cusp and hyperbolic umbilic caustics of micrometer-scale spheroids. Employing the vector ray tracing, Yu et al. [28] studied the optical caustics structures around the first rainbow angle of spheroidal water droplets, which includes the rainbow and hyperbolic umbilic fringes. And the relation between the oblateness (aspect ratio) of spheroidal droplets and the curvature of rainbow fringes is established. In the present study, the generalized rainbow techniques for characterizing the spheroidal water droplet in terms of refractive index, equatorial diameter, and aspect ratio are reviewed.

Experimental investigation

To observe the generalized rainbow patterns, an ultrasonic acoustic levitator is used to suspend a water droplet (see Fig. 1). The droplet's aspect ratio a/c is defined as the ratio of its major and minor axes - a being the diameter in horizontal equatorial plane and c the diameter measured along the symmetric axis; and the droplet can be deformed to different aspect ratio through adjusting the acoustic pressure. To measure the generalized rainbow pattern, the droplet is illuminated with vertically polarized and horizontally propagating He-Ne laser light with a wavelength of 632.8 *nm*. A CCD camera is positioned in the first rainbow region, i.e. around 138^{o} for a water droplet, and is focused at infinity so that the recorded light scattering pattern is equivalent to that observed in the far field [12]. To directly observe the droplet shape for later comparison, the droplet image is recorded by anther CCD camera with backlighting.

Figure 2a shows a nearly spherical water droplet with a=1.68 *mm* and a/c=1.03, which is recorded by camera 1 (see Fig. 1). The corresponding rainbow pattern is shown in Fig. 2b. The horizontal scattering angle θ increases from left to right. The salient feature is that the bows in Fig. 2b are almost straight lines vertical to the horizontal plane. A water droplet having a=1.59 *mm* and a/c=1.23 and the relevant generalized rainbow pattern are shown in Figs. 2c and d respectively. It can be seen that the bows in Fig. 2d become noticeably bent and the cusp caustics appears at right of this figure. The evolution process of the bows' shape as the result the droplet deformation reveals the possibility of measuring the oblateness of droplets from the curvature of the corresponding generalized rainbow fringes.

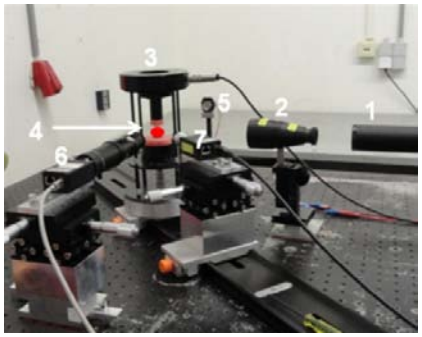

Fig.1: Experimental setup used for generalized rainbow measurement. (1) He-Ne laser, (2) beam expander, (3) ultrasonic acoustic levitator, (4) water droplet, (5) background light, (6) camera 1 focused on droplet, (7) camera 2 focused at infinity.

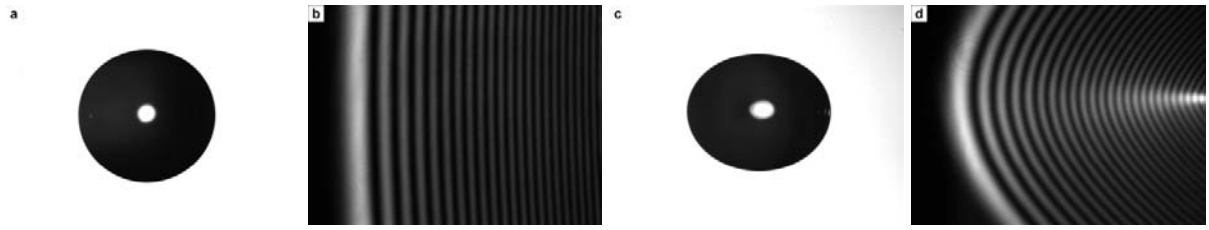

Fig. 2: Droplet images and the corresponding generalized rainbow patters: a) a=1.68 *mm* and *a/c*=1.03. c) *a*=1.59 *mm* and *a/c*=1.23.

Principle of generalized rainbow technique

By comparing the intensity distribution on the equatorial plane of the measured generalized rainbow pattern and that simulated by Airy theory, it is demonstrated that Airy theory can be used to calculate the intensity distribution from spheroidal water droplets on the equatorial plane [10]. Figure 3 displays the simulation and experimental results for water droplets, in which the experimental result is filtered to remove the ripple structures and the two results have been normalized to the same maximum value. It can be seen from the comparison that the experimental results agree well with the Airy simulation in the scattering angle region $137.50^{o}<\theta<140^{o}$. The first and second extreme values on the intensity distribution are denoted by θ_1 and θ_2 respectively. According to Airy theory, the relation between the rainbow angle, θ_1 and θ_2 is given by [29]

$$\theta_{rg} = \left(\theta_1 - c\theta_2\right)/(1-c) \qquad (1)$$

where c is a constant defined by $c=\alpha_1/\alpha_2$, (α_1=1.0874, α_2=3.4668). The parameters α_1 and α_2 can be calculated from the Airy integral [29]. After knowing θ_1 and θ_2, the rainbow angle can be calculated and then the refractive index can be inferred. Based on geometric optics, the relation between the rainbow angle and the refractive index is given as [10,29]

$$\theta_{rg} = \pi + 2\cos^{-1}\left(\frac{m_{GRP}^2-1}{3}\right)^{1/2} - 4\cos^{-1}\left(\frac{4\left(m_{GRP}^2-1\right)}{3m_{GRP}^2}\right)^{1/2} \qquad (2)$$

To evaluate the accuracy of refractive index m_{GRP} of water droplet calculated from the corresponding generalized rainbow pattern, the error Δ_m is defined as

$$\Delta_m = m_{GRP} - m \qquad (3)$$

The diameter a_{GRP} of water droplet in the equatorial plane can be calculated by [10]

$$a_{GRP} = \frac{\lambda}{4}\left[\left(\frac{3\left(4-m_{GRP}^2\right)^{1/2}}{\left(m_{GRP}^2-1\right)^{3/2}}\right)^{1/2}\left(\frac{\alpha_1-\alpha_2}{\theta_1-\theta_2}\right)^{3/2}\right] \quad (4)$$

For evaluating the precision of a_{GRP} calculated from the corresponding generalized rainbow pattern, the relative error Δ_a is given by

$$\Delta_a = \left(a_{GRP}-a\right)\times 100/a \quad (5)$$

here a is the diameter of the droplet in the equatorial plane measured by direct imaging with CCD camera.

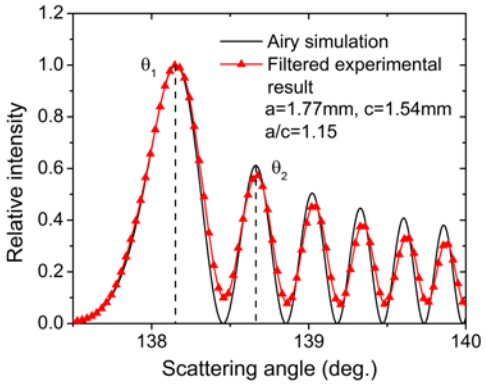

Fig. 3: Comparison of intensity distribution calculated by Airy theory with the filtered experimental result for a water droplet with a=1.77 *mm* and a/c=1.15.

As shown in Fig.2, the change of the bows' shape (rainbow fringes) of the generalized rainbow patterns as the result of droplet deformation reveals the possibility of measuring the oblateness of the droplets from the curvature of the corresponding rainbow fringes. A comparison of the curvature of fringes obtained from a vector ray tracing (VRT) simulation and that from experiments for water droplets is shown in Fig. 4a. The principle of VRT can be found in Refs. [28]. As is the convention for comparison, only the curvature at the apex point of the rainbow fringe is calculated. The curvatures calculated from the experimental rainbow patterns are shown with error bars corresponding to one standard deviation. It can be seen that the agreement between the VRT model and measurement is excellent at most aspect ratios: most deviations are within the experimental uncertainty. Attention has to be paid to the fact that, for large aspect ratio (e.g. a/c>1.23), the droplet vibrates significantly in the levitator and the relevant generalized rainbow pattern becomes highly instable and blurry. It is difficult to distinguish the rainbow fringe without using a high- speed camera. For this reason the curvature of the rainbow fringes are shown only for droplets with aspect ratio a/c≤1.23. Figure 4b plots the droplet aspect ratio against the curvature of the corresponding rainbow fringes simulated by VRT model, which reveals that the aspect ratio of droplet can be calculated based on the curvature of the rainbow fringe measured from experiment and relation between the aspect ratio and curvature shown in Fig.4 b. For a measured generalized rainbow pattern, the corresponding rainbow fringe can be calculated; then the curvature of the rainbow fringe can be obtained; finally the aspect ratio of the relevant water droplet can be inverted according to Fig. 4b.

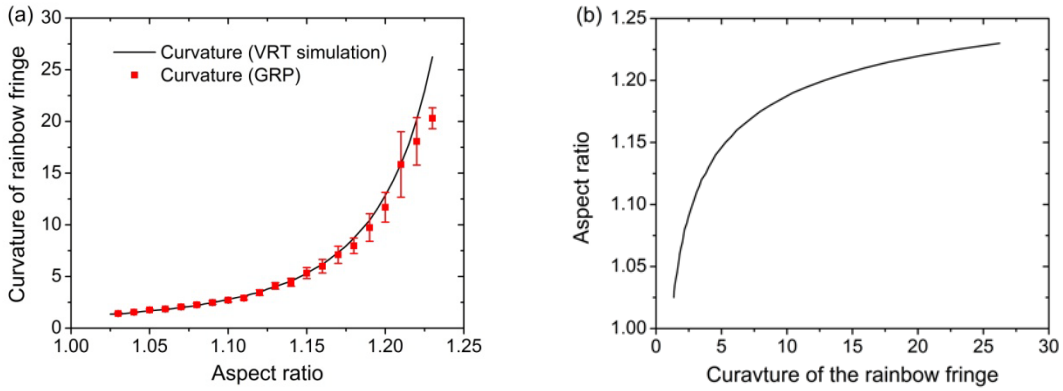

Fig. 4: (a) Comparison the curvatures of the rainbow fringes calculated from VRT simulations and that from generalized rainbow patterns for water droplets. (b) The relation between aspect ratios of water droplets and curvatures of the corresponding rainbow fringes calculated from VRT simulations.

Droplet parameters inversion

According to Eqs. (1) and (2), the refractive indices of water droplets are calculated from the generalized rainbow patterns and are shown in Fig. 5a. And the refractive indices inverted from rainbow patterns are shown with error bars corresponding to one standard deviation. It can be seen that the inverted refractive indices agree with that of pure water (*m*=1.333 at λ=632.8 *nm*). Water droplets have been studied in the range of 0.80-2.00 *mm* and aspect ratios smaller than 1.23, since smaller or larger droplets or droplets with larger ratios are unstable in the levitator. Figure 5b displays the errors of refractive indices inverted from generalized rainbow patterns. It can be seen that the absolute errors of inverted refractive indices are smaller than 0.5×10^{-4}.

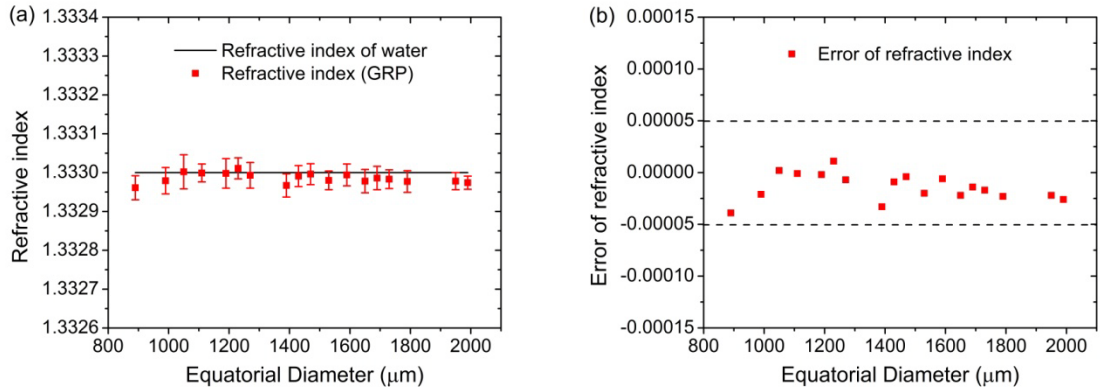

Fig. 5: (a) Refractive index of pure water droplet and that calculated from the generalized rainbow patterns. (b) Errors of refractive indices inverted from the generalized rainbow patterns.

Figure 6a displays the droplet diameters in the equatorial plane calculated by Eq. (4), in which the droplet diameters are also shown with error bars relevant to one standard deviation. It can be seen that the inverted droplet diameters are consistent with those obtained directly from the droplet image. According to Eq. (5), the relative errors for droplet diameters inverted from the generalized rainbow patterns are calculated and shown in Fig. 6b. The relative errors lie between -5% and 5%; hence reliable droplet diameter estimations can be obtained from the generalized rainbow patterns.

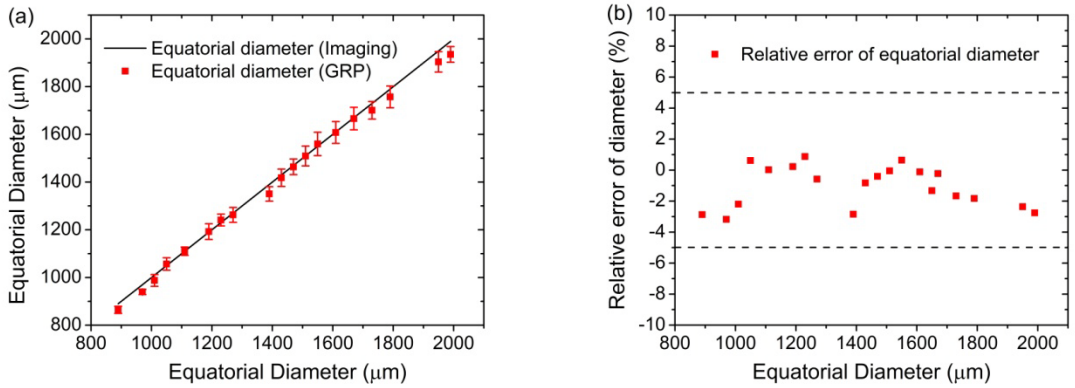

Fig. 6: (a) Water droplet diameters in the equatorial plane measured by imaging and that calculated from the generalized rainbow patterns. (b) Relative errors of droplet diameters inverted from the generalized rainbow patterns.

Based on the relation between the aspect ratio and the curvature of rainbow fringe (Fig. 4b), the aspect ratio (r_{GRP}) of the water droplet can be inverted from the generalized rainbow patterns and is compared with observed value from the directly recorded droplet image. Figure 7a gives such a comparison. The aspect ratios inverted from the generalized rainbow patterns are also shown with error bars relevant to one standard deviation. It reveals that the inverted droplet aspect ratios agree well with that from direct imaging. To evaluate the accuracy of inverted aspect ratio, the relative errors in percentage ((Δ=(r_{GRP} - $r_{Imaging}$)x100/ $r_{Imaging}$) are shown in Fig. 7b. The relative errors lie between -1% and 1%, which indicates good measurement accuracy of droplet non-sphericity (in terms of aspect ratio) from the generalized rainbow patterns.

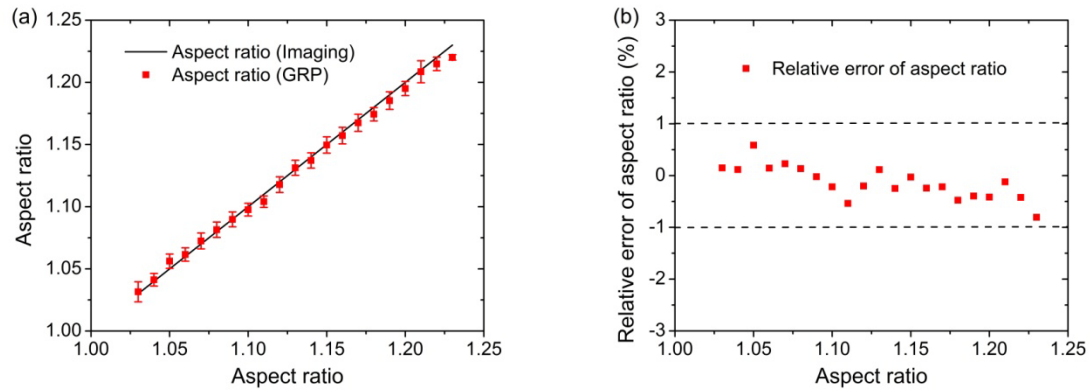

Fig. 7: (a) Comparison of water droplet aspect ratios observed from direct imaging and that inverted from the generalized rainbow patterns. (b) Relative errors of inverted aspect ratios from the generalized rainbow patterns.

Conclusion

In summary, the generalized rainbow patterns from spheroidal water droplets are measured in experiment. According to the generalized rainbow patterns and Airy theory, the refractive index and equatorial diameter of water droplets can be inverted from the corresponding generalized rainbow patterns. Comparison of the refractive indices inverted from the generalized rainbow patterns with that of pure water shows good agreement with absolute errors less than 0.5×10^{-4}. The water droplet diameters in the horizontal equatorial plane are calculated from the generalized rainbow patterns and compared to that measured by direct imaging. It is shown that the relative errors of droplet diameters associated with the generalized

rainbow patterns lie between -5% and 5%; hence reliable diameter estimations of droplets can be obtained from the generalized rainbow patterns. The curvatures of simulated rainbow fringes are compared with observed ones from the generalized rainbow patterns, in which good agreement is also shown. Since for a given type of droplet, the curvatures of the rainbow fringes are only a function of the aspect ratios, the non-sphericity (in terms of aspect ratio) of water droplets are inferred from the relevant generalized rainbow patterns. The relative errors of aspect ratios calculated from the generalized rainbow pattern lie between -1% and 1%. Accordingly, complete information of a spheroidal water droplet in terms of geometric and optical properties is obtained.

Acknowledgment

This research is supported by the German Research Foundation under Grant No. TR 194/49-1. H. Yu is also grateful to the Graduate School Computational Engineering and the Research Training Group GRK 1114 at the Technische Universität Darmstadt for supporting his Ph.D. program.

References

1. Tropea C., 2011: “Optical particle characterization in flows”, Ann. Rev. Fluid Mech. 43, pp. 399-426.
2. Albrecht H.-E., Borys M., Damaschke N., and Tropea C., 2003: “Laser Doppler and phase Doppler measurement techniques”, Heidelberg: Springer-Verlag.
3. Maeda M., Kawaguchi M., and Hishida K., 2000: “Novel interferometric measurement of size and velocity distributions of spherical particles in fluid flows”, Meas. Sci. Technol. 11, pp. L13-L18.
4. Semidetnov N., 1985: “Investigation of laser Doppler anemometer as instrumentation for two-phase flow measurements”, Doctoral dissertation (Leningrad Inst Precis Mech Opt).
5. Damaschke N., Nobach H., Semidetnov N., and Tropea C., 2002: “Optical particle sizing in backscatter”, Appl. Opt. 41, pp. 5713-5727.
6. Roth N., Anders K., and Frohn A., 1996: “Size insensitive rainbow refractometry: theoretical aspects”, Lisbon: 8th Int. Symp. Appl. Laser Techn. to Fluid Mech. pp. 9.2.1-9.2.6.
7. van Beeck J. P. A. J., Giannoulis D., Zimmer L., and Riethmuller M. L., 1999: “Global rainbow thermometry for droplet-temperature measurement”, Opt. Lett. 24, pp. 1696-1698.
8. van Beeck J. P. A. J., Zimmer L., and Riethmuller M. L., 2001: “Global rainbow thermometry for mean temperature and size measurement of spray droplets”, Part. Part. Syst. Charact. 18, pp.196–204.
9. Vetrano M. R., van Beeck J. P. A. J., and Riethmuller M. L., 2004: “Global rainbow thermometry: improvements in the data inversion algorithm and validation technique in liquid-liquid suspension”, Appl. Opt. Vol. 43, pp. 3600-3607.
10. Yu H. T., Xu F., and Tropea C., 2012: “Spheroidal droplet measurements based on generalized rainbow patterns”, J. Quant. Spectosc. Radiat. Transfer, (posted 26 September 2012, in press).
11. Berry M. V. and Upstill C., 1980: “Catastrophe optics: morphologies of caustics and their diffraction patterns”, Prog. Opt. 18, pp. 257-346.
12. Marston P. L. and Trinh E. H., 1984: “Hyperbolic umbilic diffraction catastrophe and rainbow scattering from spheroidal drops”, Nature 312, pp. 529-531.
13. J. F. Nye, 1984: “Rainbow scattering form spheroidal drops—an explanation of the hyperbolic umbilic foci”, Nature 312, pp. 531-532.
14. Marston P. L., 1985: “Cusp diffraction catastrophe from spheroids: generalized rainbows and inverse scattering”, Opt. Lett. 10, pp. 588-590.

15. P. L. Marston, “Transverse cusp diffraction catastrophes: some pertinent wave fronts and a Pearcey approximation to the wave field”, J. Acoust. Soc. Am. 81, pp. 226–232 (1987).
16. P. L. Marston, C. E. Dean, and H. J. Simpson, “Light scattering from spheroidal drops: exploring optical catastrophes and generalized rainbows”, AIP Conf. Proc. 197, pp. 275–285 (1989).
17. Dean C. E. and Marston P. L., 1991: “Opening rate of the transverse cusp diffraction catastrophe in light scattered by oblate spheroidal drops”, Appl. Opt. 30, pp. 3443-3451.
18. P. L. Marston, “Geometrical and catastrophe optics methods in scattering”, Phys. Acoust. 21, pp. 1–234 (1992).
19. P. L. Marston, “Catastrophe optics of spheroidal drops and generalized rainbows”, J. Quant. Spectosc. Radiat. Transfer, 63, pp. 341-351 (1999).
20. Nye J. F., 1992: “Rainbows from ellipsoidal water drops”, Proc. R. Soc. Lond. A 438, pp. 397-417.
21. Simpson H. J. and Marston P. L., 1991: “Scattering of white light from levitated oblate water drops near rainbows and other diffraction catastrophes”, Appl. Opt. 30, pp. 3468-3473.
22. Kaduchak G., Marston P. L., and Simpson H. J., 1994: “E_6 diffraction catastrophe of the primary rainbow of oblate water drops: observations with white-light and laser illumination”, Appl. Opt. 33, pp. 4691-4696.
23. Kaduchak G. and Marston P. L., 1994: “Hyperbolic umbilic and E_6 diffraction catastrophes associated with the secondary rainbow of oblate water drops: observations with laser illumination”, Appl. Opt. 33, pp. 4697-4701.
24. Marston P. L. and Kaduchak G., 1994: “Generalized rainbows and unfolded glories of oblate drops: organization for multiple internal reflections and extension of cusps into Alexander’s dark band”, Appl. Opt. 33, pp. 4702-4713.
25. D. S. Langley and P. L. Marston, 1998: “Generalized tertiary rainbow of slightly oblate drops: observations with laser illumination”, Appl. Opt. 37, pp. 1520-1526.
26. J. A. Lock and E. A. Hovenac,1991: “Internal caustic structure of illuminated liquid droplets”, J. Opt. Soc. Am. A8, pp. 1541–1552.
27. Lock J. A. and Xu F., 2010: “Optical caustics observed in light scattered by an oblate spheroid”, Appl. Opt. 49, pp. 1288-1304.
28. Yu H. T., Xu F., and Tropea C., 2013: “Optical caustics associated with the primary rainbow of oblate droplets: simulation and application in non-sphericity measurement”, Opt. Express, submitted.
29. van de Hulst, H. C., 1981: “Light scattering by small particles”, Dover.